

# Search for PSR B1951+32 with the GLAST LAT



D. Parent, D. Dumora, L. Guillemot, M. Lemoine-Goumard, T. Reposeur, D.A. Smith

Université Bordeaux 1; CNRS/IN2P3;  
Centre d'Etudes Nucléaires de Bordeaux Gradignan, UMR 5797,  
Chemin du Solarium, BP120, 33175 Gradignan, France

on behalf of the GLAST Mission Team



## Abstract

PSR B1951+32 has the hardest spectrum of the six pulsars seen clearly in GeV gamma rays with EGRET, with no indication of a spectral break. The diffuse gamma background in the Cygnus region where it is located is so high that it is the only EGRET pulsar that was not also listed as an unpulsed source in the 3rd catalog. These two properties make it an especially useful case to explore the selection cuts used to enhance the signals from gamma ray emitters observed with the GLAST Large Area Telescope (LAT). It is also a remarkable object to improve our understanding of gamma ray pulsars : the high cut-off energy is attributed to its relatively low magnetic field, and the particle acceleration processes are believed to be strongly influenced by the surrounding supernova remnant CTB80. The poster will present Monte Carlo simulation results that illustrate both the instrumental and physics challenges offered by PSR B1951+32.

## PSR B1951+32, the prediction of Mr Strom

The radio pulsar PSR B1951+32 was discovered by Kulkarni et al. (1988) and Clifton et al. in the core of the galactic SNR CTB80, as suggested by Strom (1987). The object is located at ~ 2 kpc with a period of 39.5 ms. Its characteristic age is  $1.1 \times 10^5$  yr, and its surface magnetic field is  $4.9 \times 10^{11}$  G. EXOSAT (1987), Einstein (1994) and ROSAT (1995) detected pulsed emission in the X-ray regime, as did RXTE more recently at hard X-ray energies (1997). PSR B1951+32 is associated with a composite supernova remnant like the Crab, making it an interesting case to study interactions between the relativistic electron/positron wind and the external medium. Furthermore, the peculiar morphology of the SNR indicates a bow shock between the PWN and the SNR ejecta (Figure 5).

Name	B1951+32
JName	J1952+3252
Galactic longitude l	68.77
Galactic latitude b	2.82
Period P	39.5 ms
Period derivative $\dot{P}$	$5.844803 \times 10^{-15}$
Distance	2.5 kpc
Characteristic age	$1.1 \times 10^5$ yrs
Surface magnetic field	$4.9 \times 10^{11}$ Gauss
Spin-down luminosity $\dot{E}$	$3.7 \times 10^{36}$ erg/s
Flux $\frac{dN}{dE}$	$3.078 \times 10^7 \text{ erg}^{1/2} \text{ s}^{-1/2} \text{ kpc}^{-2}$
Association	SNR CTB80

Table 1: Characteristics of PSR B1951+32

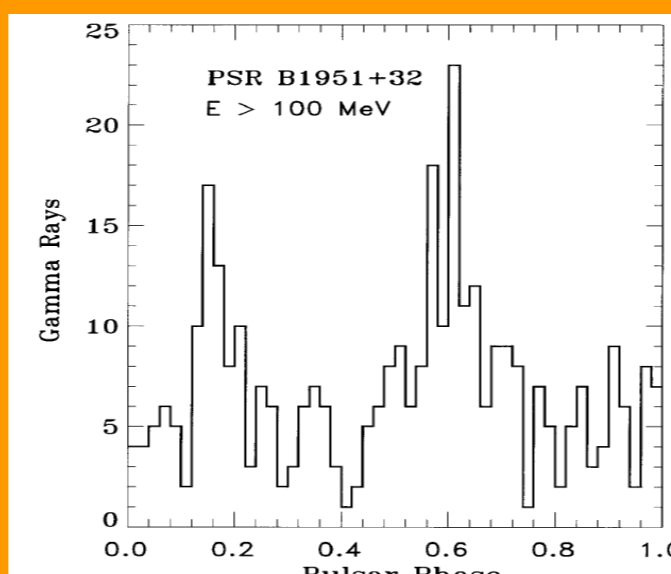


Figure 1. Light curve of the 344 gamma rays at  $E > 100$  MeV within a fixed  $1^\circ$  radius circle around PSR B1951+32. The radio peak occurs at phase 0.0 [13].

PSR B1951+32 was the sixth gamma-ray pulsar detected by EGRET [13] and was seen by COMPTEL [10] above 0.75 MeV, with a hard spectrum. The EGRET data don't show an indication of a spectral break but the upper limits of the CELESTE and Whipple telescopes impose one (figure 4).

## Pulsar spectrum simulation

### Simulation parameters :

We have simulated the spectrum of PSR B1951+32 for the first year scanning survey observations using the GLAST Science Tools, as a power law with an exponential cutoff (eqn. 1). The background includes both galactic and extragalactic diffuse gammas. LAT event selection is the DC2 standard cuts (class AB) and the current estimates of the instrument response. The pulsar flux is fixed at  $1.6 \times 10^{-7}$  ph/cm<sup>2</sup>/s [13].

### Determination of the simulated parameters by likelihood analysis :

Figure 2 represents the differential gamma ray rate of the diffuse background and the pulsar, determined by a likelihood analysis for a region of interest of 0.5 deg and energy interval of [100 MeV–100 GeV]. The green and black lines are the extragalactic and galactic background fits, respectively. The blue line is a power law fit with an exponential cutoff convoluted with the instrument response and the pink line is the sum of the three components. The red triangles represent the data. The resulting flux is  $(1.71 \pm 0.15) \times 10^{-7}$  ph/cm<sup>2</sup>/s and the energy cutoff obtained is  $31.9 \pm 9$  GeV. The fit results agree with the initial parameters. The large uncertainty on the energy cutoff of PSR B1951+32 is due to low statistics at high energies.

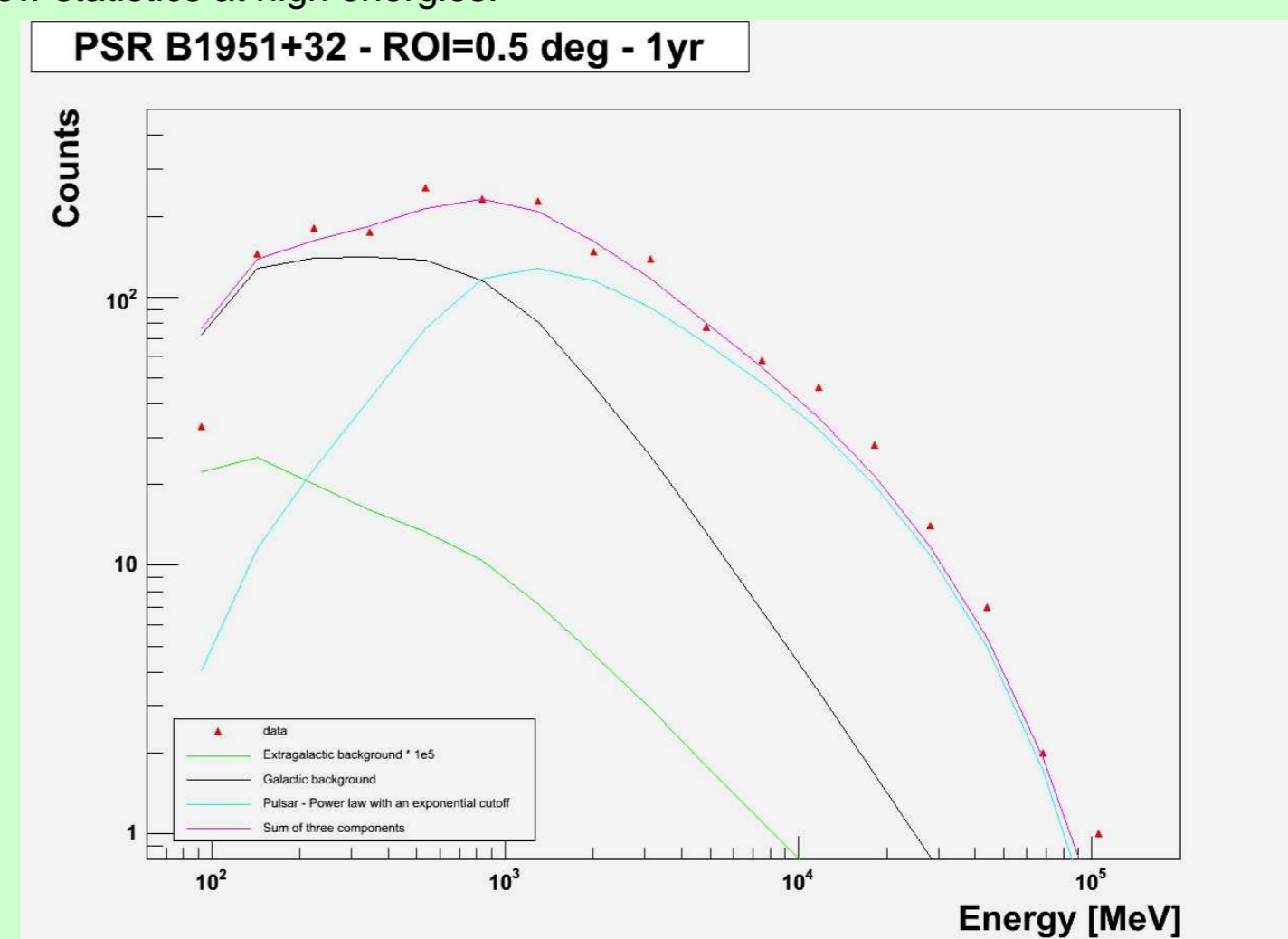


Figure 2. Differential energy spectrum of simulated PSR B1951+32. The region of interest is 0.5 degree. The green and black lines are the extragalactic and galactic background fits, respectively. The blue line is a power law with an exponential cutoff convoluted with the instrument response. The pink line is the sum of the three components. The red triangles represent the data.

## High-energy cutoff : an important feature of pulsar models

The six pulsars observed by EGRET show evidence of a high-energy turnover. This physical parameter is an important feature of pulsar models. For PSR B1951+32, the EGRET observations determined only a lower limit to the cutoff energy, which may be associated with its relatively low magnetic field (figure 3). We make the assumption based on the EGRET data and the upper limit of the CELESTE and Whipple Cherenkov telescopes, of a power law attenuated by an exponential cutoff (figure 4).

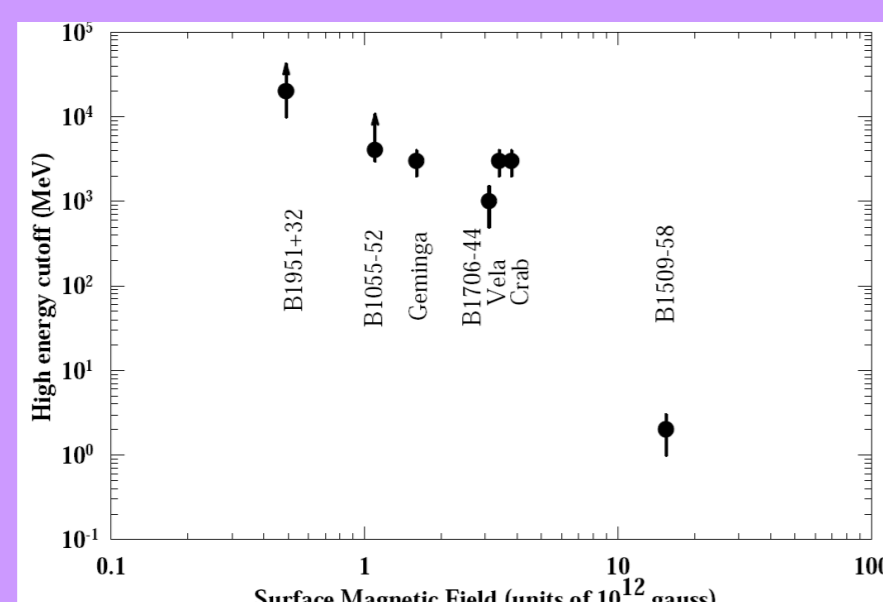


Figure 3. High-energy cutoff energy for gamma-ray pulsars as a function of surface magnetic field. For PSR B1951+32, only a lower limit to the cutoff energy can be determined from the EGRET data (Thompson – 2003).

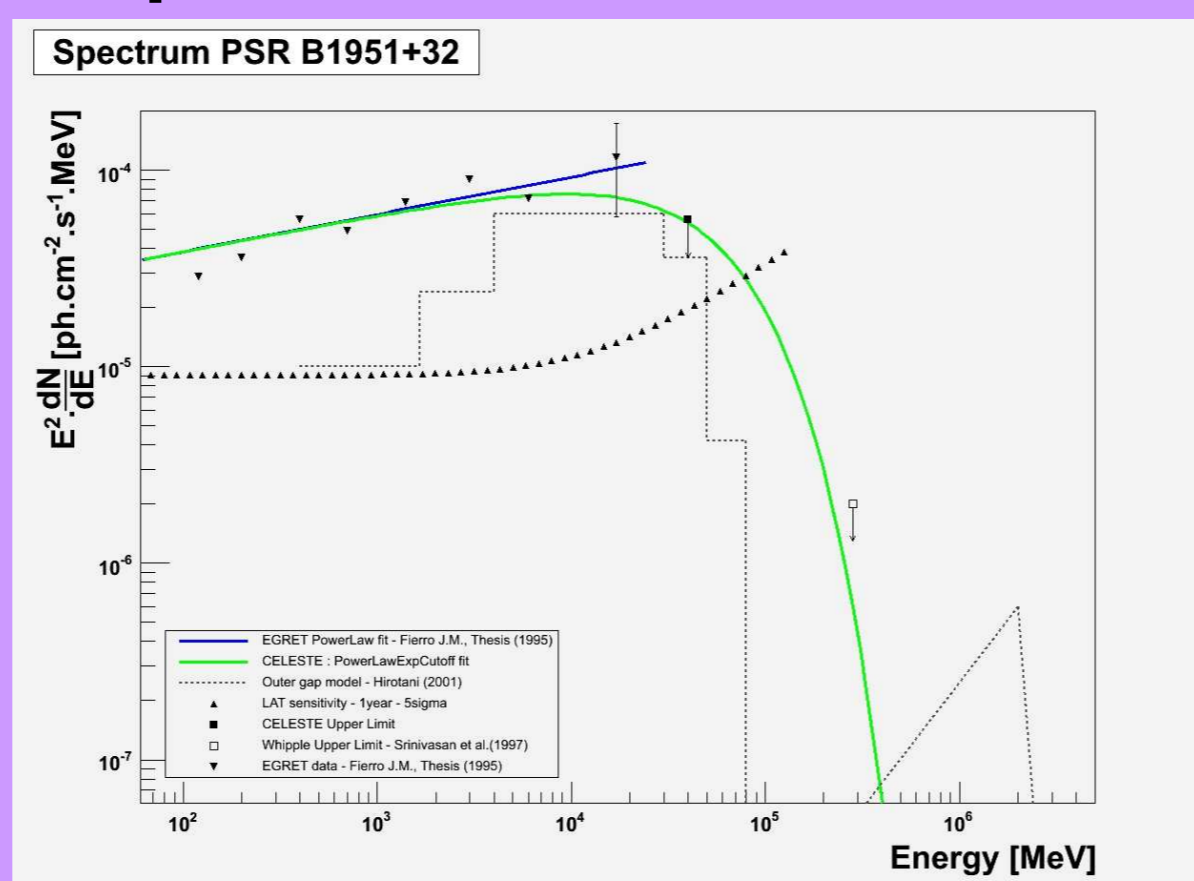


Figure 4. Pulsed energy spectrum of PSR B1951+32. The blue line represents the power-law fit to the EGRET points. The green line represents the power-law with an exponential cutoff taken from the CELESTE upper limit (Durand 2003). The dot-dashed line represents an outer gap prediction (Hirotani 2001).

The green line is the power-law with an exponential cutoff fit, based on the EGRET and CELESTE data.

$$\frac{dN}{dE} = 1.84 \times 10^{-10} (E/537\text{MeV})^{-1.81} \exp(-E/49800) \text{ ph/cm}^2\text{s/MeV (eqn. 1)}$$

## The supernova remnant CTB 80 in the $\gamma$ -ray range

PSR B1951+31 is located in the core of the supernova remnant (SNR) CTB 80. Multi-wavelength observations [4] both in the radio and X-ray band shows that the SNR consists of a plerionic and a shell-like component. The latter is an old shell, in the radiative cooling phase, comprised of three faint 30' long emission ridges. The former component, a diffuse nebula, is produced by the interaction of the pulsar relativistic wind with the external medium. The X-ray brightness [15] of the plerion in CTB 80 is orders of magnitude smaller than the Crab Nebula which should result in an inefficient self-synchrotron Compton process since the density of synchrotron photons is low. However, the electrons of the nebula, accumulated during the pulsar lifetime, can scatter soft photons (mostly CMB photons but also galactic and infra-red photons) to  $\gamma$ -ray energies.

A simple one-zone inverse-compton model [1] can be used to explain the observed radio and X-ray data shown in the table. Assuming that electrons are injected in the nebula with a total energy of  $10^{49}$  ergs (in reasonable agreement with the energy content observed in relativistic electrons) and a spectral index of 2.5, a gamma-ray flux somewhat under  $10^{-12}$  erg cm<sup>-2</sup> s<sup>-1</sup> is expected at 1 GeV. This flux is near the sensitivity limit of GLAST-LAT for one year of observations and is slightly lower than the flux predicted by Bednarek et al. [3] using a time-dependent radiation model of plerions. These two different estimates make CTB 80 a good candidate for GLAST.

Distance (kpc)	Age (kyrs)	Size ('))	X-ray flux (0.1 – 2.4 keV) (ergs s <sup>-1</sup> )	Radio flux (49 cm) (Jy)	Magnetic field (μG)
2.5	$1.1 \times 10^5$	5	$1.8 \times 10^{38}$	2.5	3.2

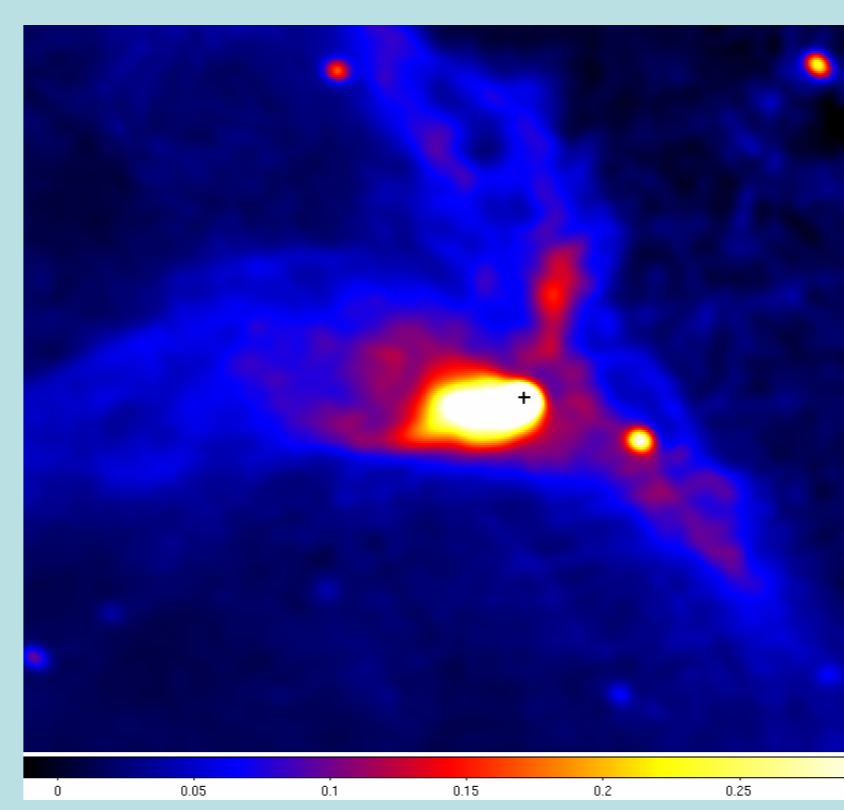


Figure 5. Radio continuum image of the SNR CTB80 at 1380 MHz, obtained from VLA observations. The black cross indicates the position of the pulsar PSR B1951+32. The scale is in units of Jy beam<sup>-1</sup>. Courtesy of Castelletti et al. [4].

## Significance study with PSR B1951+32

Although not listed as an unpulsed source in the Third EGRET catalog, due to the high background in the Cygnus region, high-energy gamma pulsation from PSR B1951+32 was clearly seen [13].

### 1 – Unpulsed excess

We find S events within 1 degree around the radio pulsar position. We estimate the background B from the number of events in a ring of 5 degrees from the pulsar, with the same area ( $\pi/4$  square degrees). For the standard cuts applied to the 55 day DC2 simulation, we obtain S = 867 and B = 513, yielding a significance of  $(S-B)/\sqrt{(S+B)} = 9.5$ , that is 1.3  $\sigma/\sqrt{\text{day}}$ . For the "loose" cuts applied to the 55 day DC2 simulation, we obtain S = 1164 and B = 705, yielding a significance of  $(S-B)/\sqrt{(S+B)} = 10.6$ , that is 1.4  $\sigma/\sqrt{\text{day}}$ .

### 2 – Pulsed excess for a known peak position

Referring to Figure 6, we define *Off* to be the number of events in the off-pulse region,  $0.85 < \phi < 1.0$ , and B to be the background normalized to the on-pulse intervals,  $B = \text{Off} \cdot 0.62 / 0.15$ . For P events in the on-pulse region, the signal S is P-B with significance  $S/\sqrt{(B)}$ . For this 1-year simulation, *Off* is 730 and P is 4960 events for the standard cuts, yielding 1.8  $\sigma/\sqrt{\text{day}}$ . Similarly, the "loose" cuts give 1.9  $\sigma/\sqrt{\text{day}}$ .

## Cut optimization for the faint source PSR B1951+32

These light curves for PSR B1951+32 model the data from Ramanamurthy et al. [13] as 2 Lorentzian peaks. The one year simulation includes the detector physics, and the spacecraft geometry and orbital motion. Charged particle backgrounds, and galactic and extragalactic diffuse gamma fluxes, are taken from the second GLAST data challenge (DC2). For DC2, standard LAT event selection cuts were defined to reject most proton background. However, in the plane of the Milky Way, after standard cuts, diffuse gammas dominate the charged particle rates significantly. Consequently, for faint sources like PSR B1951+32, we can « loosen » the cuts to increase the number of gamma rays from the source without decreasing the signal significance (figure 6). The diffuse gamma rate is still ~5x higher than the residual proton background.

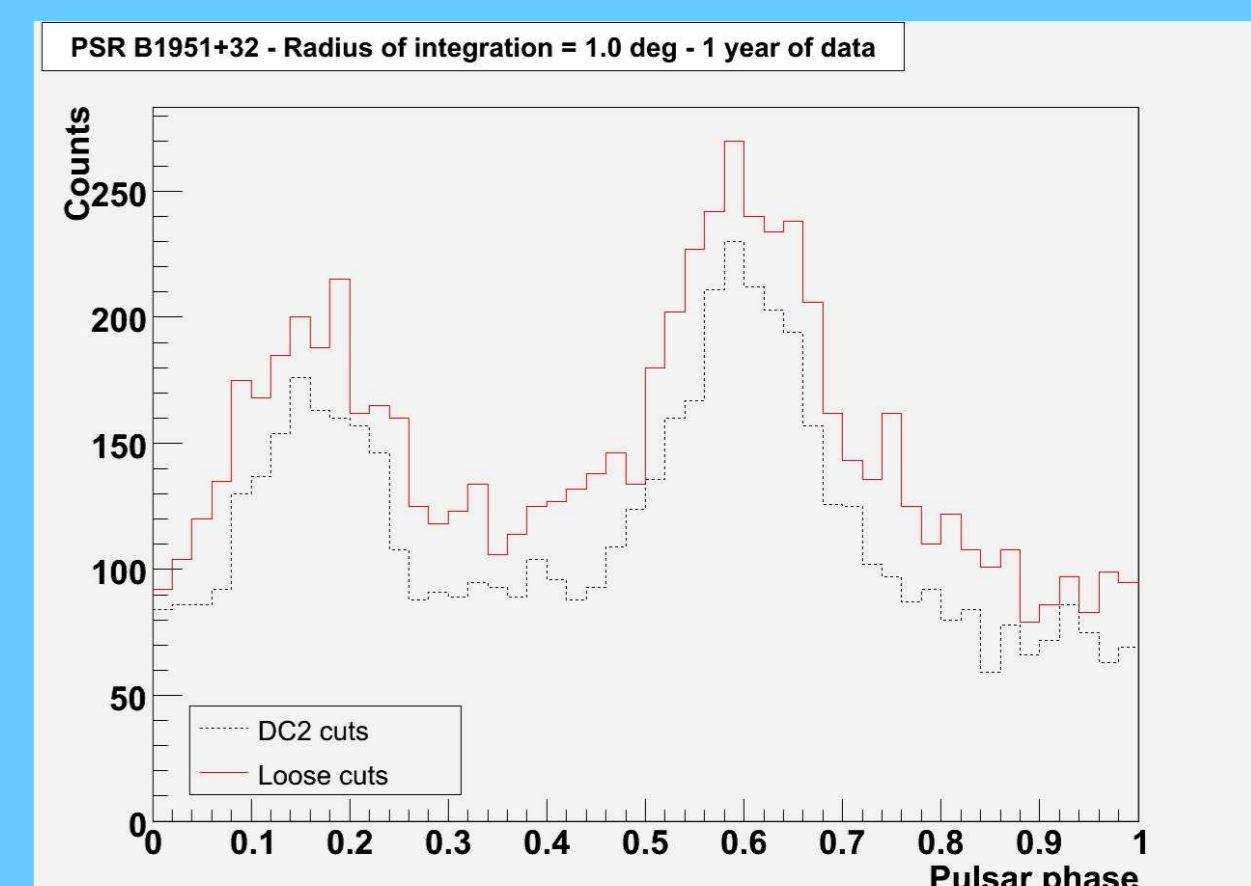


Figure 6. Phase distribution of PSR B1951+32, assigning phase ranges 0.12-0.22, 0.48-0.74 and 0.22-0.48 to the first and second peaks, and the bridge, respectively. The dashed light curve uses the standard DC2 cuts. The red light curve uses the « loose » cuts.

12% more  $\gamma$ -rays kept with the loose cuts with the same significance.

### DC2 cuts :

S = 1941 & B = 3019  
Sig = 35  $\sigma$  per  $\sqrt{\text{year}}$

### Loose cuts :

S = 2315 & B = 3959  
Sig = 37  $\sigma$  per  $\sqrt{\text{year}}$

(S, B defined in "significance" frame)

## REFERENCES

- Aharonian F., Atoyan A., Kifune T., MNRAS, 291, 162 (1997)
- Ballet J., Selection of an optimal band to report fluxes, LAT-SAP-TN-0001 (2005)
- Bednarek W. and M. Bartosik A&A 405, 689-702 (2003)
- Castelletti G., Dubner G., A&A 440, 171-177 (2005)
- Chang, H.-K., Ho, C., ApJ 479, L125 (1997)
- Cheng, L., Li, T., Sun, X., et al., Ap&SS 213, 135 (1994)
- Clifton, T. R. et al. IAU Circ. No. 4422 (1987)
- Durand E., Recherche de photons pulsés au-dessus de 30 GeV dans le Crabe et PSR B1951+32 avec le détecteur Cerenkov atmosphérique CELESTE, Thesis (2003)
- Hirotani, K. and Shibata S., AS, 325, 1228 (2001)
- Kuiper, L. et al. A&A, 337, 421 (1998)
- Kulkarni, S. R., et al., Nature, 331, 50 (1988)
- Ogelman, H., Buccheri, R., A&A 186, L17 (1987)
- Ramanamurthy, P. V., et al., ApJ, 447, L109 (1995)
- Strom, R. G., ApJ, 319, L103 (1987)
- S. Safi-Harb and H. Ogelman ApJ 439, 722-729 (1995)
- Thompson D. J., arXiv:astro-ph/0312272 v1 Gamma ray pulsars (2003)